

Exact solutions for viscous Marangoni spreading

Thomas Bickel¹ and François Detcheverry²

¹*Univ. Bordeaux, CNRS, Laboratoire Ondes et Matière d'Aquitaine, F-33400 Talence, France*

²*University of Lyon, Université Claude Bernard Lyon 1, CNRS, Institut Lumière Matière, F-69622 Villeurbanne, France*

(Dated: September 13, 2022)

When surface-active molecules are released at a liquid interface, their spreading dynamics is controlled by Marangoni flows. Though such Marangoni spreading was investigated in different limits, exact solutions remain very few. Here we consider the spreading of an insoluble surfactant along the interface of a deep fluid layer. For two-dimensional Stokes flows, it was recently shown that the non-linear transport problem can be exactly mapped to a complex Burgers equation [Crowdy, *SIAM J. Appl. Math.*, **81**, 2526 (2021)]. We first present a very simple derivation of this equation. We then provide fully explicit solutions and find that varying the initial surfactant distribution – pulse, hole, or periodic – results in distinct spreading behaviors. By obtaining the fundamental solution, we also discuss the influence of surface diffusion. We identify situations where spreading can be described as an effective diffusion process but observe that this approximation is not generally valid. Finally, the case of a three-dimensional flow with axial symmetry is briefly considered. Our findings should provide reference solutions for Marangoni spreading, that may be tested experimentally with fluorescent or photoswitchable surfactants.

I. INTRODUCTION

The spreading of surface-active species at aqueous interfaces is a long-standing issue in interfacial science [1]. Surfactants, of which amphiphilic molecules are the prime example, accumulate at interfaces where they lower the surface tension [2]. As a consequence, a gradient in surface concentration induces a Marangoni stress at the interface [3, 4]. Inhomogeneities in the distribution of surfactants thus drive a liquid flow, that in turn couples with the surfactant distribution. This complex feedback mechanism may eventually lead to the rigidification of the interface that can alter the rising motion of gas bubbles [5–8]. Another striking effect observed in microfluidic experiments is that traces of surfactants can severely limit the drag reduction of superhydrophobic surfaces [9–11]. More generally, Marangoni stresses due to the presence of surfactants, even at a very low concentration, are ubiquitous through fundamental processes [12–14], the natural world [15–17] and industrial applications [18]. The consequences are essential for a variety of phenomena, including film thickness in coating [19], dispersion relation for capillary waves [20] and stability of foams [21, 22].

The dynamics of surfactant spreading is also relevant in the field of active matter through the propulsion mechanism of Marangoni swimmers [23–25]. When a particle filled with surface-active molecules such as camphor is placed at the air-water interface, the resulting surface-tension gradient drives the spontaneous motion of the particle, even if the latter is perfectly symmetric [26–28]. Although camphor swimmers are known for centuries [27], their rich individual and collective dynamics is still a matter of investigation [29–32]. To elucidate their propulsion mechanism, a fine understanding of the transport of surfactants is required. In particular, it has been suggested both experimentally [33] and

theoretically [34, 35] that the transient spreading of camphor molecules could be described by an effective diffusion process that would account for the advection by the Marangoni flow. This point is actually quite subtle and requires an in-depth investigation.

When a surfactant is released at the air-liquid interface, the surfactant-covered domain grows in time and its size $L(t)$ is governed by a balance between viscous stresses and surface tension gradients. At large time, the size generally follows the scaling law $L(t) \sim t^\alpha$. The exponent α depends on the dominant features of the system such as inertia, gravity, capillarity or viscous dissipation, among others. Although most of previous studies focused on thin films [36–40], where the lubrication approximation applies, we consider here the deep layer limit. Regarding the dynamics of surfactant spreading, asymptotic self-similar solutions have been thoroughly discussed in the wake of the seminal work of Jensen [41]. More recently, the hydrodynamic signature of surfactant transport in a semi-infinite liquid has also been investigated at steady state [42–45]. This line of works focuses mainly on the large Reynolds limit, where the surfactant-driven flow develops in a boundary layer.

In contrast, much less is known regarding the properties of Marangoni spreading with Stokes flow. In this case, the vorticity created by the Marangoni shear stress at the interface penetrates deep into the liquid, so that the transport equations are generally both nonlocal and nonlinear [1]. An important step forward was achieved, however, when it was recognized that the interfacial velocity can be expressed as a convolution of the surface concentration [46]. Another essential finding, achieved recently by Crowdy [47], has revealed that the mathematical problem for insoluble surfactant can be mapped to a complex Burgers equation, opening new perspectives for its resolution.

The aim of the present work is to exploit those ad-

vances to build a complete set of exact solutions for viscous Marangoni spreading. In contrast to self-similar solutions that apply asymptotically, our solutions are valid at all time. We find that the non-linear character of the spreading problem leads to a rich variety of possible behaviors and that the initial surfactant distribution has a key influence on the subsequent evolution. Besides, our exact solutions provide reference cases and a range of physical insights. In particular, the question of Marangoni spreading as an effective diffusion process can now be settled.

The study is organized as follows. In Sec. II, we first present the hydrodynamic model with its underlying assumptions and propose a particularly simple derivation of the complex Burgers equation that governs the dynamics of insoluble surfactants in one dimension. Section III focuses on transient Marangoni spreading in the absence of diffusion. Exact solutions are obtained for a variety of initial surfactant distributions. The influence of surface diffusion is investigated in Sec. IV, where we provide a fundamental solution and discuss the resulting effective diffusion coefficient. Finally, we examine in Sec. V the spreading dynamics in two dimensions with axial symmetry. We conclude in Sec. VI with a physical discussion of our findings.

II. FROM MARANGONI SPREADING TO BURGERS EQUATION

A. Dimensionless numbers and simplifying assumptions

We consider the spreading of surfactants at the air-water interface, as illustrated in Fig. 1. Initial inhomogeneities in the surfactant distribution induce Marangoni constraints and a fluid flow that drives the system toward a homogeneous state. Our goal is to provide an exact description of this relaxation process. We assume a two-dimensional flow and an infinitely deep liquid layer. The liquid is Newtonian and incompressible, with dynamic viscosity η , mass density ρ and kinematic viscosity $\nu = \eta/\rho$. The surface-active molecules are insoluble, i.e. they are irreversibly adsorbed at the interface. We note D_s their surface diffusion coefficient.

To introduce further modeling assumptions, we first discuss the relevant dimensionless numbers. The contribution of advection to momentum and mass transport can be rationalized by the Reynolds and Péclet numbers

$$\text{Re} \equiv \frac{LU}{\nu} \quad \text{and} \quad \text{Pe} \equiv \frac{LU}{D_s}, \quad (1)$$

with L the length scale of the initial concentration perturbation and U the velocity associated with the corresponding Marangoni flow. Both quantities may span a large range in experiments, namely $L = 10^{-3} - 10^{-1}$ m and $U = 10^{-3} - 1$ m s $^{-1}$, resulting in Reynolds number $\text{Re} = 1 - 10^5$ much above or around unity. Because

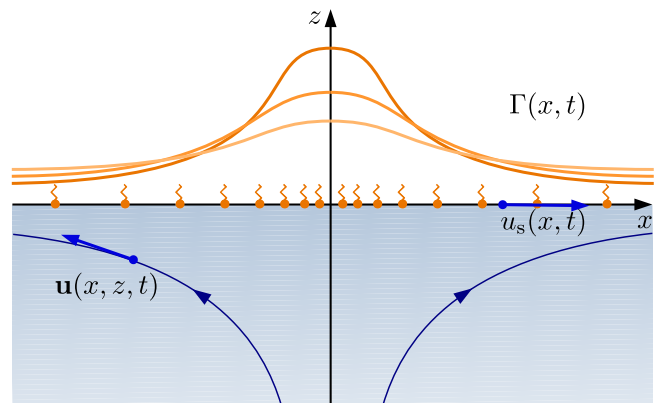


FIG. 1. Spreading of an insoluble surfactant above a semi-infinite liquid layer with two-dimensional flow. The inhomogeneous distribution of surfactant $\Gamma(x, t)$ induces a Marangoni flow with bulk velocity $\mathbf{u}(x, z, t)$ and interfacial velocity $u_s(x, t)$.

the surface diffusion coefficient $D_s \simeq 10^{-9}$ m 2 s $^{-1}$ [48] is several orders of magnitude smaller than the momentum transport coefficient $\nu \simeq 10^{-6}$ m 2 s $^{-1}$, the hierarchy $\text{Re} \ll \text{Pe}$ always applies [49]. The thickness of the hydrodynamic boundary layer is therefore much larger than that of the mass boundary layer [43]. In the following, we neglect fluid inertia and focus on the Stokes regime. This assumption is reasonable when L lies below or within the millimeter range and U in the mm s $^{-1}$ range at most. While this choice of the Stokes limit is certainly restrictive, we will show in the following that it is interesting in its own right. Emphasis is placed on nonlinearities that occur in the mass transport equation and on the methods to handle them exactly.

The spreading of surfactant can induce an unsteady displacement of the free interface. The competition between surface deformation and viscous stress is quantified by the capillary number

$$\text{Ca} \equiv \frac{\eta U}{\gamma}, \quad (2)$$

with γ the surface tension of the interface. With $\eta \simeq 10^{-3}$ Pa s, $\gamma = 10^{-2} - 10^{-1}$ N m $^{-1}$ and the range of velocity scale given above, one gets $\text{Ca} = 10^{-5} - 10^{-1}$. We can therefore neglect capillary effects and assume that the interface remains flat in the formulation of the hydrodynamic problem. Still, interfacial deformations can be determined afterward by invoking the normal stress continuity condition [41].

Finally, some surface-active species such as camphor or alcohol molecules may evaporate from the liquid to the gas phase. To account for this phenomenon, we include a first-order kinetic evaporation with rate k . The ratio of evaporative to convective mass transport is set by the Damköhler number

$$\text{Da} \equiv \frac{kL}{U}, \quad (3)$$

that can take values in a very wide range, spanning from negligible ($Da \ll 1$) to prevalent ($Da \gg 1$) evaporation.

B. Marangoni flow and surfactant transport

In the viscous regime, the velocity field $\mathbf{u} = (u, v)$ and pressure p satisfy the incompressible Stokes equations

$$\nabla \cdot \mathbf{u} = 0, \quad \eta \Delta \mathbf{u} = \nabla p, \quad (4)$$

with ∇ the nabla operator and Δ the Laplacian. The velocity is assumed to vanish far away from the initial disturbance. Along the free interface, variations in surface tension γ induce a tangential stress given by the Marangoni boundary condition

$$\eta \partial_z u|_{z=0} = -\partial_x \gamma, \quad (5)$$

where the interface remains flat and corresponds to $z = 0$. The surface tension is related to the local surfactant concentration Γ through an equation of state $\gamma = \gamma_o - \kappa \Gamma$ that is linear [50], a convenient but approximate assumption [40, 51]. Surface activity is then measured by the positive constant $\kappa \equiv -\partial \gamma / \partial \Gamma$. Finally, the concentration $\Gamma(x, t)$ of surfactant evolves according to the advection-diffusion equation

$$\partial_t \Gamma + \partial_x (\Gamma u_s) = D_s \partial_{xx}^2 \Gamma - k \Gamma, \quad (6)$$

where $u_s(x, t) \equiv u(x, z = 0, t)$ is the velocity at the interface. The last term in Eq. (6) accounts for evaporation.

C. Closure relation and Thess' equation

Since the Stokes equation is linear, it should be possible to relate the flow anywhere in the bulk to the distribution of Marangoni stress at the interface, and thus ultimately to the distribution of surfactant. This step has indeed been achieved by Thess and collaborators [46, 49, 52] (see also Ref. [53]). The end result is a closure relation giving the surface velocity as a convolution of surfactant concentration with a dimension-dependent kernel. When the surface velocity is one-dimensional, the closure relation reads

$$u_s(x, t) = \frac{\kappa}{2\eta} \mathcal{H}[\Gamma(x, t)]. \quad (7)$$

Here, we define the Hilbert transform \mathcal{H} of a function f

$$\mathcal{H}[f](x) \equiv \check{f}(x) \equiv \frac{1}{\pi} \text{p.v.} \int_{-\infty}^{\infty} \frac{f(x')}{x - x'} dx', \quad (8)$$

where the integral is understood in the sense of Cauchy principal value (p.v.). The closure relation of Eq. (7) is non-local: the velocity at position x depends on the surfactant distribution everywhere on the surface. This is

in clear contrast with the thin layer limit, where the surface velocity is simply proportional to the concentration gradient $\partial_x \Gamma$ [49].

It is convenient at this point to switch to dimensionless variables. From now on, we focus on the reduced surfactant concentration $f = \Gamma/\Gamma_o$ and the reduced velocity $u = u_s/U$, with Γ_o the concentration scale and $U = \kappa \Gamma_o / 2\eta$ the characteristic velocity associated with the Marangoni flow. The length and time scales are also expressed in units of L and $\tau = L/U$, with L the relevant size pertaining to the initial perturbation. Expecting no confusion by the reader, we keep the same notations x and t for the dimensionless variables. According to Eq. (7), the closure relation in dimensionless form simply reads $u(x, t) = \check{f}(x, t)$.

Putting all pieces together, the flow and surfactant dynamics described by Eqs. (4)–(6) can finally be replaced by a unique equation originally introduced by Thess [52]

$$\partial_t f + \partial_x (f \check{f}) = -\alpha f + \epsilon \partial_{xx}^2 f, \quad (9)$$

where α and ϵ stand respectively for the Damköhler number $\alpha \equiv Da$ and the inverse Péclet number $\epsilon \equiv Pe^{-1}$. By “integrating out” the features of the flow, the coupled problem of momentum and mass transport is reduced to a single equation, which is, however, nonlinear and non-local.

D. Complex Burgers equation

Although some specific solutions of Thess' equation have been discussed previously in the literature [35, 49, 52, 53], a systematic method for solving the problem is still missing. A major breakthrough has been achieved very recently by Crowdy [47], recognizing that the problem defined by Eqs. (4)–(6) can be mapped to a complex Burgers equation. The derivation is based on the complex variable representation of the stream function and therefore relies on advanced properties of analytic functions. Here we propose a different route, inspired by an approach originally developed in the context of vorticity transport [54].

By exploiting properties of Hilbert transforms, let us show that Crowdy's result can be derived in a straightforward manner. The first step is to apply the Hilbert operator to Eq. (9) to obtain

$$\partial_t \check{f} + \check{f} \partial_x \check{f} - f \partial_x f = -\alpha \check{f} + \epsilon \partial_{xx}^2 \check{f}. \quad (10)$$

Here, we made use of the relations $\mathcal{H}[\partial_x f] = \partial_x \check{f}$, $\mathcal{H}[fg] = \check{f}g + f\check{g} + \mathcal{H}[\check{f}\check{g}]$ and $\mathcal{H}^2[f] = -f$, from which one also gets $\mathcal{H}[f\check{f}] = (\check{f}^2 - f^2)/2$ [54, 55]. The second step is to introduce the complex function $\Psi(x, t)$ as

$$\Psi(x, t) \equiv \check{f}(x, t) - if(x, t). \quad (11)$$

Combining Eqs. (9) and (10), it is then a simple calculation to recover Crowdy's equation [47]

$$\partial_t \Psi + \Psi \partial_x \Psi = -\alpha \Psi + \epsilon \partial_{xx}^2 \Psi, \quad (12)$$

with an additional term that accounts for evaporation. This equation expresses that in the present setting, Marangoni spreading is formally governed by a viscous Burgers equation for the complex function $\Psi(x, t)$. If a solution can be found, the interfacial velocity and the concentration are deduced from

$$u(x, t) = \text{Re}[\Psi(x, t)], \quad f(x, t) = -\text{Im}[\Psi(x, t)]. \quad (13)$$

Note that, since f is a concentration, it should always satisfy $f(x, t) \geq 0$.

The inverse Péclet number ϵ appearing in Eq. (12) plays the role of viscosity in the more common form of the Burgers equation, which was initially introduced in the context of fluid turbulence [56, 57]. The effect of evaporation is embodied through an extra linear term monitored by the Damköhler number α . The main accomplishment of shifting from Thess' to Crowdy's formulation is that locality is now restored in the Burgers Eq. (12). Moreover, a rigorous mathematical transformation allows to further transform the nonlinear Burgers equation into a linear partial differential equation [58]. As a consequence, analytical solutions for the transient spreading of insoluble surfactants can be derived and discussed in a systematic way. We now proceed to do so.

III. TRANSIENT SPREADING AT INFINITE PÉCLET NUMBER

The situation most amenable to analytical treatment is when diffusion and evaporation are both absent ($\alpha = \epsilon = 0$ or $\text{Da} = \text{Pe}^{-1} = 0$). The equation to solve in this case is the inviscid Burgers equation [56, 57, 59]

$$\partial_t \Psi + \Psi \partial_x \Psi = 0. \quad (14)$$

If $\Psi_o(x) \equiv \Psi(x, 0)$ denotes the initial value, the solution given by the method of characteristics [60] is simply

$$\Psi(x, t) = \Psi_o(x^*), \quad \text{with} \quad x^* + t\Psi_o(x^*) = x. \quad (15)$$

It remains only to solve the equation on x^* . We have identified five relevant cases where this is possible: two types of surfactant ‘‘pulses’’, two types of surfactant ‘‘holes’’ and one periodic distribution.

A. Spreading dynamics of surfactant pulses

Cauchy pulse. We first assume that the initial profile is a Cauchy (or Lorentzian) distribution with amplitude \mathcal{A} and width a . The initial values are then

$$f_o(x) = \frac{\mathcal{A}a^2}{a^2 + x^2}, \quad \text{and} \quad \check{f}_o(x) = \frac{x}{a} f_o(x), \quad (16)$$

so that $\Psi_o(x) = a\mathcal{A}/(x + ia)$. Given the simplicity of the expressions, Eq. (15) reduces to a second order equation for x^*

$$x^{*2} - (x - ia)x^* + \mathcal{A}at - iax = 0, \quad (17)$$

which leads to the solution

$$\Psi(x, t) = \frac{1}{2t} \left(x + ia - i \left[(a - ix)^2 + 4a\mathcal{A}t \right]^{1/2} \right). \quad (18)$$

Separating the real and imaginary parts [61], the concentration and velocity profiles are obtained explicitly as

$$f(x, t) = \frac{1}{2t} (\Upsilon^+(\xi) - a), \quad (19a)$$

$$u(x, t) = \frac{1}{2t} (x - \Upsilon^-(\xi)), \quad (19b)$$

where we define $\xi \equiv a^2 + 4a\mathcal{A}t - x^2$ and

$$\Upsilon^\pm(\xi) \equiv \sqrt{\left(\sqrt{\xi^2 + (2ax)^2} \pm \xi \right)} / 2. \quad (20)$$

To keep compact expressions, we have assumed $x > 0$. The negative part can be obtained by symmetry since $f(x, t)$ and $u(x, t)$ are respectively even and odd with respect to x . The resulting concentration and velocity profiles are shown in Fig. 2(a).

Circular pulse. As a second instance, we consider an initial surfactant profile that is elliptical or ‘‘circular’’ after rescaling:

$$f_o(x) = \mathcal{A} \left[1 - x^2/a^2 \right]_+^{1/2}, \quad (21a)$$

$$\check{f}_o(x) = \frac{\mathcal{A}}{a} \left(x - [x^2 - a^2]_+^{1/2} \right), \quad (21b)$$

with radius a and amplitude \mathcal{A} . The brackets $[\cdot]_+$ indicate the positive part of the argument. Here we also assume $x > 0$ for the sake of brevity. The initial values lead to $\Psi_o(x) = (\text{sign}(a - x)\sqrt{a^2 - x^2} + ix)\mathcal{A}/a$. Equation (15) is again second order for x^* and proceeding as above, the concentration and velocity profiles then read

$$f(x, t) = \frac{a\mathcal{A}}{a(t)} \left[1 - \frac{x^2}{a^2(t)} \right]_+^{1/2}, \quad (22a)$$

$$u(x, t) = \frac{a\mathcal{A}}{a^2(t)} \left(x - [x^2 - a^2(t)]_+^{1/2} \right), \quad (22b)$$

where $a(t) = \sqrt{a^2 + 2a\mathcal{A}t}$. The circular solution, plotted in Fig. 2(b), is self-similar. Indeed, Eq. (22) shows that the profile at any time can be obtained by replacing the initial radius a with a time-dependent radius $a(t)$, while keeping a fixed amount of surfactant. In the context of Marangoni spreading, the circular solution was initially found by Thess [52] with an adhoc method. In the mathematical literature [62], it is known as a fundamental solution which arises when assuming self-similarity. Note that like other self-similar solutions, such as the Barenblatt-Pattle solution for the porous medium equation [63, 64], the circular pulse solution has a finite support.

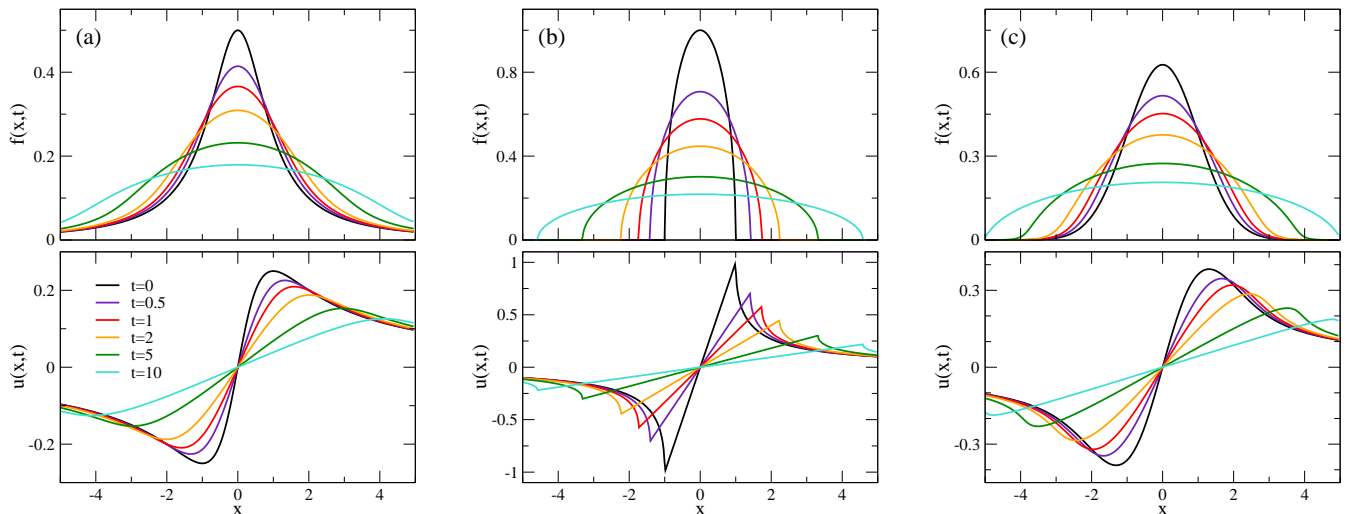


FIG. 2. Spreading of a surfactant pulse: Concentration and velocity profiles for a Cauchy, circular and Gaussian pulse, from left to right. The typical width is $a = 1$ and the total amount of surfactant is the same in all cases. Time is $t = 0, 0.5, 1, 2, 5, 10$ from top to bottom. Note that the vertical scale changes from one graph to the other.

More general pulse shapes. The Cauchy and circular pulses are special because they both lead to a second order equation for Eq. (15). Other pulse shapes yield an equation on x^* that in general cannot be solved explicitly [65]. Still, it is always possible to resort to numerical resolution. The example of a Gaussian pulse treated this way is shown in Fig. 2(c). In the limit $t \rightarrow \infty$, all pulses eventually approach the fundamental circular solution [66]. However, it is apparent that such loss of memory of the initial profile happens only at long time, for $t \simeq 10$ in dimensionless units. This indicates that the shape of the initial pulse has a significant influence on transient Marangoni spreading.

Effective diffusion coefficient. We now examine whether the spreading process can be described as an effective diffusion process, as suggested in several studies [33, 34, 67]. For the circular pulse, the spatial extension squared $a^2(t) = a^2 + 2aAt$ increases linearly with time, a feature typical of diffusion. But for the Cauchy pulse, the second moment of the concentration profile is infinite so that the width of the surfactant distribution is not properly defined. One can use instead the position $x_{v\max}$ where the velocity is maximal. In the large time limit, one finds $x_{v\max} \simeq 2\sqrt{aAt}$, a behavior again reminiscent of diffusion. An effective diffusion coefficient can thus be defined as $D_{\text{eff}} \sim aA$. Interestingly, D_{eff} is proportional to the total amount of surfactant in the pulse. Thus, the more surfactant in the pulse, the faster the spreading. Such a feature, which would not be permitted with plain diffusion since the corresponding equation is linear, is a consequence of nonlinearity. Surfactant spreading may thus be described as a diffusive process, but only under specific circumstances and with regard to the time evolution of the concentration profile.

B. Closure dynamics of surfactant holes

We now discuss the reverse situation where surfactant is already present at the interface but with a concentration near the origin that is lower than the value \bar{c} far away from it. Such surfactant “dimple” or for brevity “hole” in the following is expected to close as a result of Marangoni flow. As for the spreading case, we derive two exact solutions for this process: the Cauchy hole and the circular hole.

Cauchy hole. Consider the initial surfactant concentration given by

$$f_o(x) = \bar{c} - \frac{a^2 \mathcal{A}}{a^2 + x^2}, \quad (23)$$

with $0 \leq \mathcal{A} \leq \bar{c}$. Retracing the steps detailed above, the Ψ function, concentration and velocity can all be written explicitly in a straightforward manner. For the sake of clarity, the mathematical expressions are reported in App. C. An interesting feature occurs when the initial concentration vanishes at the origin, i.e. when $\mathcal{A} = \bar{c}$. In this case, the concentration profile exhibits a singularity at a finite time $t^* = a/\bar{c}$. Indeed, a small- x expansion gives at lowest order

$$x \rightarrow 0, \quad f(x, t^*) = -\frac{u(x, t^*)}{\text{sign}(x)} = \frac{\bar{c}}{\sqrt{2a}} \sqrt{|x|}. \quad (24)$$

This indicates that the concentration profile has a cusp near the origin, as illustrated in Fig. 3(a). Regarding the velocity profile, it has an infinite slope at the origin when $t = t^*$. For larger time $t > t^*$, the profile becomes regular again. Note that this singularity has already been identified in previous investigations [47], but focusing on the dynamics of poles in the complex plane. For $\bar{c} = \mathcal{A}$,

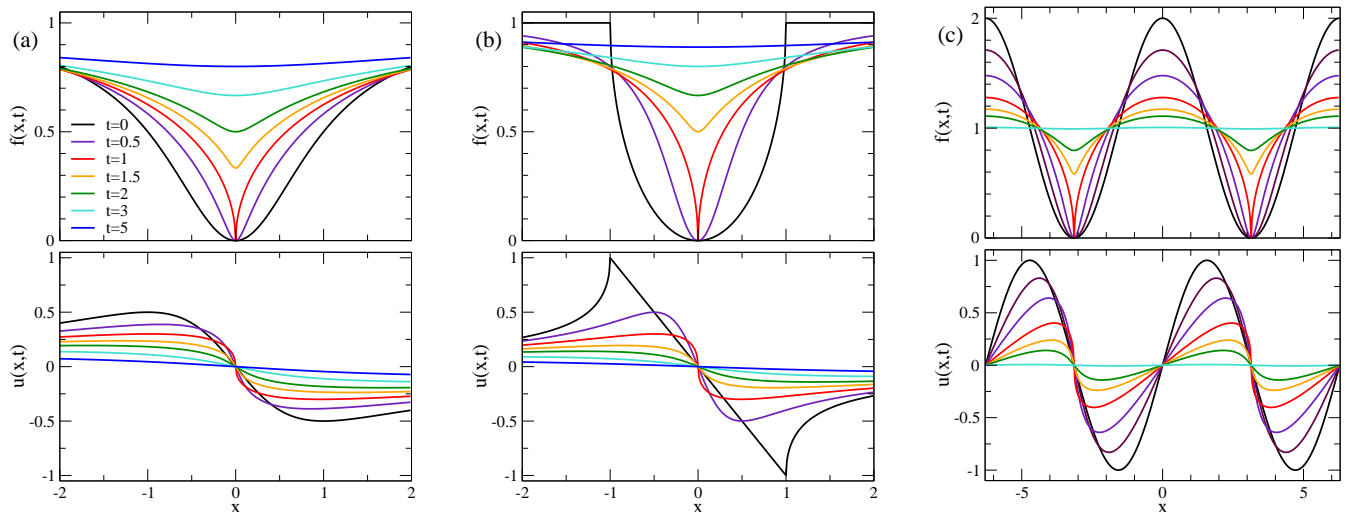


FIG. 3. (a-b) Closing of a surfactant hole: Concentration and velocity profiles for Cauchy and circular holes. Here $\bar{c} = a = \mathcal{A} = 1$. Time is $t = 0, 0.5, 1, 1.5, 2, 3, 5$ from bottom to top. A singularity occurs at $t^* = 1$ and $x^* = 0$. (c) Relaxation of a periodic distribution of surfactant: Concentration and velocity profiles for a sinusoidal initial distribution, with $\bar{c} = a = \mathcal{A} = 1$. Time is $t = 0, 0.2, 0.5, 1, 1.5, 2, 5$. A singularity occurs at $t^* = 1$ and $x^* = \pm\pi$.

the concentration at the origin has a remarkably simple expression

$$t \leq t^*, \quad f(0, t) = 0, \quad (25a)$$

$$t \geq t^*, \quad f(0, t) = \bar{c} \left(1 - \frac{t^*}{t}\right). \quad (25b)$$

The concentration remains zero until the cusp forms at time t^* , after which it relaxes as t^{-1} .

Circular hole. The case of an elliptic initial dimple can also be treated analytically. The initial density reads

$$f_o(x) = \bar{c} - \frac{\mathcal{A}}{a} [a^2 - x^2]_+^{1/2}, \quad (26)$$

with the condition $0 \leq \mathcal{A} \leq \bar{c}$. The exact solution is provided in App. C. The concentration and velocity profiles are displayed in Fig. 3(b). When $\mathcal{A} = \bar{c}$, the concentration exhibits a finite-time singularity as well, with features similar to those discussed above. In particular, Eq. (24) still holds, with the factor of 2 removed. Regarding the concentration at the origin, one now gets

$$t \leq t^*, \quad f(0, t) = 0, \quad (27a)$$

$$t \geq t^*, \quad f(0, t) = \bar{c} \left(1 - \frac{t^*}{2t - t^*}\right). \quad (27b)$$

We therefore find that the concentration relaxes asymptotically with the same t^{-1} law.

C. Periodic distribution of surfactant

We now turn to a periodic initial distribution of surfactant with sinusoidal variations of period $2\pi a$ and amplitude \mathcal{A} around the mean value \bar{c} [68]. From $f_o(x) =$

$\bar{c} + \mathcal{A} \cos(x/a)$ and $i\Psi_o(x) = \bar{c} + \mathcal{A} \exp(ix/a)$, the solution can be found as

$$i\Psi(x, t) = \bar{c} + \frac{a}{t} W \left(\frac{t\mathcal{A}}{a} \exp[(ix - \bar{c}t)/a] \right), \quad (28)$$

where W is the principal value of the Lambert function that satisfies $W(x) \exp[W(x)] = x$ [69]. The corresponding profiles are plotted in Fig. 3(c). Once again, if the initial concentration includes a point of vanishing concentration (i.e. $\mathcal{A} = \bar{c}$), the profile exhibits a singularity at $(t^*, x^*) = (1, \pm\pi a)$ with the same features as discussed previously. As a side remark, we note that the solution of Eq. (28) derived for an infinite system also applies to a finite domain $x \in [-\pi a, \pi a]$ with no-flux boundary conditions.

The asymptotic behavior can also be extracted from Eq. (28). In the large-time limit, the relaxation is found to be exponential

$$t \rightarrow \infty, \quad f(x, t) - \bar{c} = \mathcal{A} \cos(x/a) e^{-t/\tau_r}. \quad (29)$$

The characteristic time $\tau_r = a/\bar{c}$ is independent of the modulation amplitude \mathcal{A} but decreases with the mean concentration \bar{c} . In other words, a surfactant-laden interface can erase initial inhomogeneities more rapidly when richer in surfactant. At this point, it is instructive to compare with a purely diffusive process. For diffusion, the relaxation of a sinusoidal profile is exponential at all time with a characteristic time $\tau_D = a^2/D$. Here, Marangoni spreading exhibits a similar behavior: setting $\tau_r = a^2/D_{\text{eff}}$, one can define an effective diffusion coefficient $D_{\text{eff}} \sim a\bar{c}$ that is again proportional to the total amount of surfactant involved, as already discussed in Sec. III A. The analogy with diffusion is, however, incomplete. As clearly seen in Fig. 3(c), the concentration profile in surfactant-poor and surfactant-rich regions evolves

in a very asymmetric manner. Such a feature, that arises from the nonlinearity of Eq. (14), would be proscribed in a diffusion process.

IV. SPREADING DYNAMICS AT FINITE DAMKÖHLER OR PÉCLET NUMBERS

When either evaporation or diffusion are relevant, additional terms have to be accounted for and the inviscid Burgers Eq. (14) has to be replaced by its more general version Eq. (12). We discuss in this section the new solutions that arise when considering finite Damköhler or Péclet numbers.

A. Effect of evaporation

For finite Damköhler number, i.e. when evaporation is considered, the equation to solve is $\partial_t \Psi + \Psi \partial_x \Psi = -\alpha \Psi$. One can easily check that the solution Ψ with evaporation ($\alpha > 0$) is directly related to the solution Ψ^\dagger without evaporation ($\alpha = 0$) by

$$\Psi(x, t) = e^{-\alpha t} \Psi^\dagger(x, \tau_{\text{eff}}), \quad \tau_{\text{eff}} = \frac{1 - e^{-\alpha t}}{\alpha}. \quad (30)$$

Note in particular that combining Eq. (30) and the circular pulse solution Eq. (22) yields back the solution obtained previously in Ref. [35].

Evaporation has two effects. First, both the concentration and the velocity include an exponential decay with rate α . Second, the effective time τ_{eff} , which is equal to t at short times $t \ll \tau_{\text{eff}}$, subsequently reaches a plateau at longer times $t \gg \tau_{\text{eff}}$. The plateau value $\tau = \alpha^{-1}$ corresponds to the characteristic time associated with evaporation. This implies that the long-time behavior of the relaxation is always exponential, whatever the initial distribution. Asymptotically, evaporation is thus the dominant transport mechanism.

B. Effect of surface diffusion

1. Fundamental solution

We come back to the situation where there is no evaporation and focus on the effect of surfactant diffusion along the interface. We assume that the interface is initially clean, with $f(x, t = 0) \rightarrow 0$ for $x \rightarrow \infty$. The equation to solve is now the viscous Burgers equation

$$\partial_t \Psi + \Psi \partial_x \Psi = \epsilon \partial_{xx}^2 \Psi, \quad (31)$$

with ϵ the inverse Péclet number which is proportional to the surface diffusion coefficient D_s . This nonlinear equation can actually be converted to a linear partial differential equation thanks to the Hopf transformation [58].

Denoting as $\Psi_o(x)$ the initial value, the general solution can be expressed as

$$\Psi(x, t) = -2\epsilon \partial_x \log I(x), \quad (32)$$

where we define

$$I(x) \equiv \int_{-\infty}^{\infty} \exp(-g(u)/\epsilon) du, \quad (33)$$

$$g(u) \equiv \frac{(u-x)^2}{4t} + \frac{1}{2} \int_0^u \Psi_o(u') du'. \quad (34)$$

This general solution is now specified for a Cauchy pulse because among the initial profiles we consider, this case is the only one we found to be fully tractable analytically. Considering the initial value $\Psi_o(x) = a\mathcal{A}/(x+ia)$, one gets

$$I(x) = \int_{-\infty}^{\infty} (1 - iu/a)^{-\frac{a\mathcal{A}}{2\epsilon}} \exp\left[-\frac{(u-x)^2}{4\epsilon t}\right] du. \quad (35)$$

While the result of the latter integral is available for any width a and amplitude \mathcal{A} [70], we focus for simplicity on the limit $a \rightarrow 0$ while keeping $a\mathcal{A} = 1/\pi$, so that the total amount of surfactant is unity. In this limit, the initial Cauchy pulse approaches a Dirac distribution. The explicit expression for $I(x)$ is then

$$I(x) = \Gamma(\zeta) {}_1F_1\left(\zeta, \frac{1}{2}, -\frac{x^2}{4\epsilon t}\right) + i \frac{2x}{\sqrt{4\epsilon t}} \Gamma\left(\frac{1}{2} + \zeta\right) {}_1F_1\left(\frac{1}{2} + \zeta, \frac{3}{2}, -\frac{x^2}{4\epsilon t}\right), \quad (36)$$

where Γ denotes here the gamma function, ${}_1F_1$ is the confluent hypergeometric function [71] and $\zeta \equiv 1/4\pi\epsilon$. Using Eq. (32), fully explicit expressions can be written for the velocity and concentration profiles. The resulting formulas then constitute the fundamental solution for Marangoni spreading with surface diffusion.

2. Effective diffusion coefficient

The primary effect of diffusion is to smooth out the distribution. This is illustrated in Fig. 4 at fixed time: the stronger the diffusion coefficient, the wider the surfactant distribution. Because the spreading of a Cauchy pulse is already diffusive-like when $\epsilon = 0$, one expects that the whole process — now including genuine surface diffusion — can be described with an effective diffusion coefficient. To do so, we focus on the concentration at the origin, which is given by the remarkably simple expression

$$f(x=0, t) = \frac{1}{\sqrt{4\pi D_{\text{eff}} t}}, \quad (37)$$

with an effective coefficient D_{eff} defined as

$$D_{\text{eff}}(\epsilon) = \pi\epsilon \left[\frac{\Gamma(1+\zeta)}{\Gamma(\frac{1}{2}+\zeta)} \right]^2, \quad \zeta \equiv 1/4\pi\epsilon. \quad (38)$$

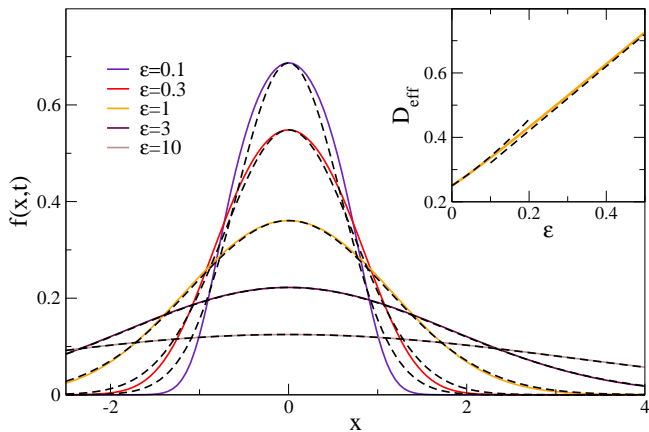


FIG. 4. Influence of surface diffusion on the transient spreading of a Dirac pulse. Here, time is fixed to $t = 0.5$ and the concentration profile is shown for $\epsilon = 0.1, 0.3, 1, 3, 10$ from top to bottom. The dashed lines correspond to Gaussian distributions with variance $2tD_{\text{eff}}(\epsilon)$. Inset: Effective diffusion coefficient $D_{\text{eff}}(\epsilon)$ as given by Eq. (38). Approximations from Eqs. (39) and (40) are also shown with dashed lines.

Equation (37) is valid at all time and matches rigorously what is expected for a purely diffusive process. A similar dependence also holds asymptotically at long time for any finite position x . The effective diffusion coefficient $D_{\text{eff}}(\epsilon)$ is plotted as a function of ϵ in the inset of Fig. 4. We can identify the limiting behaviors

$$\epsilon \rightarrow 0, \quad D_{\text{eff}}(\epsilon) = \frac{1}{4} \left(1 + \pi\epsilon + \frac{\pi^2}{2}\epsilon^2 + \dots \right), \quad (39)$$

$$\epsilon \rightarrow \infty, \quad D_{\text{eff}}(\epsilon) = \epsilon + C_1, \quad (40)$$

where $C_1 \approx 0.22$ is a numerical constant [72]. One thus recovers the expected values in two limits. For very weak diffusion $\epsilon \ll 1$, the value of the effective coefficient approaches $D_{\text{eff}} = 1/4$, in agreement with Eq. (19a) for the zero-diffusion case [73]. On the other hand, one obtains $D_{\text{eff}} \simeq \epsilon$ when intrinsic diffusion dominates. Finally, since a Gaussian behavior is expected for pure diffusion, the concentration profiles can be compared to Gaussian distributions with variance $2tD_{\text{eff}}(\epsilon)$, as done in Fig. 4. Though small discrepancies are visible in the tails of the distributions, the agreement is fairly good. The fundamental solution of Marangoni spreading may thus be reasonably approximated as a diffusive process with effective coefficient $D_{\text{eff}}(\epsilon)$ given by Eq. (38).

We have focused so far on surfactant spreading in the transient regime. Yet another situation of interest is when the surfactant is released continuously [34, 42, 43, 45, 74, 75]. We describe in App. A the solutions that are available for this steady state source in the one-dimensional case.

V. AXIALLY SYMMETRIC SPREADING IN TWO DIMENSIONS

A. Closure relation and Riesz transform

In this section, we briefly discuss transient surfactant spreading in higher dimensionality. Evaporation and diffusion are discarded everywhere. Space dimensionality is noted D and the dimension of the interface is $d = D - 1$. Keeping the assumptions made in Sec. II, the closure relation of Eq. (7) can be generalized in any space dimension as [49]

$$\mathbf{u}_s(\mathbf{x}) = -\nabla(-\Delta)^{-1/2}f(\mathbf{x}), \quad (41)$$

or, equivalently, in Fourier representation

$$\hat{\mathbf{u}}_s(\mathbf{q}) = -\frac{i\mathbf{q}}{q}\hat{f}(\mathbf{q}). \quad (42)$$

Here, \mathbf{u}_s denotes the in-plane velocity at the interface, \mathbf{x} is the position along the interface and $\hat{f} \equiv \mathcal{F}[f]$ is the Fourier transform of a function f [76]. For the dimension $d = 1$ discussed until now, the velocity is given by the Hilbert transform of the concentration. For the dimension $d = 2$ considered in this section, the velocity can be expressed as the Riesz transform of the concentration, $\mathbf{u}_s = \mathcal{R}[f]$, where we define

$$\mathcal{R}[f](\mathbf{x}) \equiv \frac{1}{2\pi} \text{p.v.} \int \frac{\mathbf{x} - \mathbf{x}'}{|\mathbf{x} - \mathbf{x}'|^3} f(\mathbf{x}') d\mathbf{x}'. \quad (43)$$

Consequently, the closure relation is again non-local.

Whereas an extensive literature can be found on Hilbert transforms, the use of Riesz transforms appears to be less common. Moreover, it does not seem possible to recast the problem as a Burgers equation. From now on, we restrict the discussion to radially symmetric pulses, such that the concentration f depends only on the distance r to the origin. Denoting as \mathbf{e}_r the radial unit vector, the velocity is also radial with component $u_r = \mathcal{R}[f] \cdot \mathbf{e}_r \equiv \check{f}$. The equation governing the evolution of surfactant distribution $f(r, t)$ is then

$$\partial_t f + \frac{1}{r} \partial_r (r f \check{f}) = 0. \quad (44)$$

Even within these assumptions, computing the Riesz transform is in general not straightforward. Several expressions that are useful for this purpose are given in App. B.

B. Transient spreading

By analogy with the one-dimensional case, we consider the spreading of a circular pulse

$$f(r, t) = \frac{a^2 \mathcal{A}}{a^2(t)} \left[1 - \left(\frac{r}{a(t)} \right)^2 \right]_+^{1/2}, \quad (45)$$

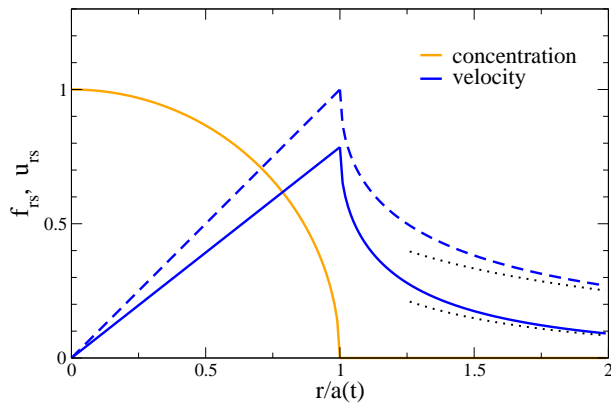


FIG. 5. Concentration and velocity profiles for the circular solution to transient spreading. Shown are the rescaled concentration $f_{rs} \equiv \lambda(t)f(r, t)$ and the rescaled velocity $u_{rs} \equiv \lambda(t)u(r, t)$, with a scaling factor $\lambda(t) = (a(t)/a)^d/\mathcal{A}$, d the dimension, $a(t)$ the radius at time t and a the initial radius. The case $d = 2$ (solid lines) and $d = 1$ (dashed line) correspond respectively to Eqs. (45)-(46) and Eq. (22). The dotted line is the large distance approximation of velocity from Eqs. (48) and (49) taken at lowest order.

where a and \mathcal{A} are respectively the initial radius and amplitude, and the time-dependent radius $a(t)$ is to be determined. Computing the Riesz transform, we get

$$\check{f}(r, t) = \frac{\pi a^2 \mathcal{A}}{4a^3(t)} r, \quad (46)$$

$$\check{f}(r, t) = \frac{a^2 \mathcal{A}}{2a^3(t)} \left[-\frac{a(t)}{r} \sqrt{r^2 - a^2(t)} + r \arcsin\left(\frac{a(t)}{r}\right) \right].$$

for $r \leq a(t)$ and $r \geq a(t)$ respectively. Equation (44) is then satisfied provided $a'(t)a^2(t) = -\pi a^2 \mathcal{A}/4$, which finally leads to

$$a(t) = \left(a^3 + \frac{3\pi a^2 \mathcal{A}}{4} t \right)^{1/3}. \quad (47)$$

We recover the self-similar solution that was identified in the mathematical literature [62] but using a completely different method. The transient spreading in the two-dimensional geometry is therefore subdiffusive, since the spatial extent increases as $a(t) \sim t^{1/3}$.

It is interesting to compare the characteristics of the circular pulse for $d = 1$ and $d = 2$. As visible in Fig. 5, both solutions have a finite support within which the velocity is linear and also feature an angular point with infinite slope at the boundary $r = a(t)$. At distances much larger than $a(t)$, the velocity behaves as

$$d = 1, \quad \frac{u(x)}{a\mathcal{A}} = \frac{1}{2x} + \frac{a^2 + 2a\mathcal{A}t}{8x^3} + \dots, \quad (48)$$

$$d = 2, \quad \frac{u(r)}{a^2\mathcal{A}} = \frac{1}{3r^2} + \frac{a^2(t)}{10r^4} + \dots \quad (49)$$

The velocity is thus proportional to the ‘‘volume’’ of the pulse $\sim a^d \mathcal{A}$ and decays as a power law $u(r) \sim r^{-d}$.

C. Steady spreading from a source

As the last solvable case, let us consider a punctual source releasing a steady flux of surfactant Q that spreads in two dimensions, without evaporation. Assuming steady state, Eq. (44) or surfactant conservation gives

$$2\pi r f(r) \check{f}(r) = Q. \quad (50)$$

Using the Riesz transform expressions of App. B, one can show that a solution is

$$f(r) = \sqrt{\frac{2}{\pi}} \frac{\Gamma(\frac{5}{4})}{\Gamma(\frac{3}{4})} \sqrt{\frac{Q}{r}}, \quad (51a)$$

$$u(r) = \sqrt{\frac{2}{\pi}} \frac{\Gamma(\frac{3}{4})}{\Gamma(\frac{1}{4})} \sqrt{\frac{Q}{r}}. \quad (51b)$$

The concentration f and the velocity $u = \check{f}$ display the same power-law dependence, a behavior clearly distinct from diffusive behavior where no steady state exists when $d = 2$. The $r^{-1/2}$ dependence might be understood from a simple argument. Since there is no characteristic length scale other than the distance to the source, one can expect a typical viscous stress $u(r)/r$. On the other hand, the typical Marangoni stress is $f'(r)$. Equating viscous and Marangoni stresses and using Eq. (50), one finds $f'(r)f(r) \sim r^{-2}$ and $f(r) \sim u(r) \sim r^{-1/2}$.

For a steady source of insoluble surfactant [44, 45], Mandre found that the velocity field decays as $r^{-\nu}$ with $\nu = 3/5$, whereas we find an exponent $\nu = 1/2$. The former applies when there is a boundary layer for the flow, the latter holds for Stokes flow. An other point of comparison is the exact solution from Bratukhin and Maurin for a steady punctual source of heat or soluble surfactant in three dimensions [77, 78], in which the far-field velocity decays as r^{-1} . Spreading of an insoluble surfactant in the Stokes regime has thus a distinct hydrodynamic signature with the slowest velocity decay.

VI. DISCUSSION

To summarize, we developed a unified analytical approach to describe the transient and steady Marangoni spreading of an insoluble surfactant in the Stokes flow limit [79]. In the one-dimensional case, the mapping between an intricate set of transport equations and a complex Burgers equation is derived in a straightforward manner using the properties of Hilbert transforms. The solutions previously uncovered in the various fields of the literature – from applied mathematics to physical chemistry through fluid mechanics – are gathered within a single framework. Importantly, our approach allows to identify all cases where a fully explicit solution is possible. By investigating a number of them, we show that the nonlinearity of the Burgers equation may lead to a variety of behaviors in spreading. Finally, for an initial surfactant distribution with arbitrary shape, the solution will

not be generally available in analytical form but may be obtained numerically by solving a simple equation. With a set of exact solutions in hands, we can now discuss more thoroughly the physical insights they provide. To do so, we consider several points in turn, focusing on the one-dimensional case if not mentioned otherwise.

Time scale for Marangoni spreading. If we switch back to dimensional variables, the time scale involved with transient surfactant spreading reads $\tau = 2\eta L/\kappa\Gamma_o$, with L the characteristic length scale of the perturbation. This time scale is thus inversely proportional to the surfactant concentration. Taking $\Gamma_o \simeq 10^3$ molecules/ μm^2 , which corresponds to a low surface fraction $\varphi \simeq 10^{-3}$, $\kappa = k_B T \simeq 4 \times 10^{-21}$ J at room temperature and the viscosity of water $\eta \simeq 10^{-3}$ Pa.s, one gets a macroscopic time $\tau \simeq 1$ s for $L = 1$ mm. Our results are thus relevant with regards to experimental time scales.

(Dis)similarities between pulses and holes. To compare the complementary situations of pulses and holes, we examine the long-time behavior of the concentration $f(x, t)$, which is normalized by the ‘‘volume’’ $a\mathcal{A}$ of the initial perturbation so that whatever the amount of surfactant, the spatial integral is unity. For any finite position x , the concentration evolves asymptotically as

$$t \rightarrow \infty, \quad \frac{f(x, t)}{a\mathcal{A}} \simeq \frac{1}{\sqrt{\chi a \mathcal{A} t}}, \quad (52)$$

for a pulse whereas for a hole

$$t \rightarrow \infty, \quad \frac{\bar{c} - f(x, t)}{a\mathcal{A}} \simeq \frac{1}{\chi \bar{c} t}, \quad (53)$$

with χ a numerical constant [80]. Two differences can be emphasized. (i) The time relaxation of pulses is essentially diffusive-like, with an effective diffusion coefficient $D_{\text{eff}} \sim a\mathcal{A}$ proportional to the total amount of surfactant in the pulse. In contrast, hole closing cannot be described as a diffusive process. (ii) The dynamics of hole closing is much faster than pulse spreading. This difference arises from the non-linear nature of the transport equation. Indeed, with a linear equation, holes and pulses would evolve in the same way. This clearly indicates that any analogy with effective diffusion has to be handled carefully.

Surfactant spreading on a contaminated surface. Our results also indicate that Marangoni spreading is very sensitive to the initial state of the surface: There is an essential difference in the behavior expected with a perfectly clean surface and a surface already covered with endogenous surfactants [81, 82]. Indeed, the solution for the holes still holds when $\mathcal{A} < 0$, that is when a surfactant pulse is released on a surface with an initial homogeneous concentration \bar{c} . In the long-time limit, the spreading dynamics thus depends on whether the interface is clean or contaminated with surface-active molecules. Such a change in behavior can be traced back to the additional term $\bar{c} \partial_x \check{f}$ appearing in Eq. (9), which describes the transport of endogenous surfactants by the Marangoni

flow due to the added surfactant pulse. Because the distribution of endogenous surfactants may become inhomogeneous, a contaminated interface with concentration \bar{c} is not equivalent to a clean interface with surface tension $\gamma_o - \kappa\bar{c}$. In particular, the asymptotic dynamics of Eq. (52) for a clean interface cannot be recovered by taking the limit $\bar{c} \rightarrow 0$ in Eq. (53). This point is especially relevant for experiments with aqueous solvents. Indeed, it may provide a clear signature of interfacial contamination that could be tested experimentally.

Mode decomposition. Whether the decay of an initial surfactant pulse can be decomposed in sinusoidal modes is a natural question. This issue has been addressed recently in a linearized version of the transport equations [83]. Here, we solved the full nonlinear equations. We note in particular that, when the amplitude of the perturbation is small with respect to mean level ($\mathcal{A} \ll \bar{c}$), the surfactant profile indeed remains sinusoidal while decaying exponentially. This is expected since this assumption makes the problem linear [84]. On the other hand, nonlinear effects become relevant as soon as \mathcal{A}/\bar{c} is not well below unity and the mode decomposition does not apply anymore.

Effective diffusion and space dimension. In the one-dimensional geometry, we have identified several cases – including surfactant pulse with and without surface diffusion – where the Marangoni spreading can be mapped to a diffusion process, though with specific features. For a two-dimensional interface, the algebra is much more involved and only two analytical solutions are so far available: the spreading dynamics for a circular pulse and the steady state source. For the former, the spreading in the long-time limit is subdiffusive with exponent 1/3. For the latter, the velocity decays as a power law, at odds with a diffusive behavior. Taken together, these findings point to the impossibility of defining an effective diffusion coefficient in the two-dimensional case. Since this situation is the most relevant experimentally, this calls for caution. Even though the idea of effective diffusion is sometimes invoked, it appears difficult, in general, to map a transport process dominated by Marangoni convection onto a simple diffusive process.

To conclude, we briefly discuss how our findings may be tested experimentally. Predictions for Marangoni spreading have long been confronted to experiments [1], using for instance fluorescent surfactants [85, 86]. To reproduce the situations considered in this work, two peculiar features are needed. First, the set-up must allow to tailor the initial profile of surfactant to a prescribed shape. Second, the one-dimensional geometry is preferable because it is best understood and amenable to complete predictions. The controlled deposition of surfactant at the interface might be a possible option. However, the use of photoswitchable surfactant molecules [87–90] could be an ideal method to induce the pulse, hole and periodic patterns that we have considered theoretically. Indeed, because the activated surfactants appear right at the interface, the perturbations are minimal. Besides,

the one-dimensional geometry is easily imposed and the concentration profile can be prescribed through the light intensity. We thus hope that the exact solutions found in this work can be put to experimental test, so as to provide, for the one-dimensional case at least, a complete picture for the viscous Marangoni spreading of an insoluble surfactant.

Appendix A: Steady release of surfactant

We seek a steady state in the plane flow geometry when the surfactant is continuously released at the surface with a distributed source profile $q(x)$. Introducing the complex flux $\mathcal{Q} = \check{q} - iq$ and neglecting diffusion, the equation to solve is now

$$\Psi \partial_x \Psi = -\alpha \Psi + \mathcal{Q}(x). \quad (\text{A1})$$

As before, the source profile more susceptible to analytical treatment is a Cauchy profile and we set $\mathcal{Q} = 1/(x + ia)$.

No evaporation. For a single Cauchy source, the solution to Eq. (A1) diverges for $x \rightarrow \infty$, suggesting that there is no steady state. Let us assume then that some local surfactant sink exists, where surfactant molecules disappear. This is physically realizable if a photoswitchable surfactant can be instantaneously disabled with a certain light. We can thus consider a source surrounded by two sinks at position $\pm l$, all of Cauchy type. The resulting steady state is described by

$$\Psi(x) = -i\sqrt{\text{Log}(l^2 + (a - ix)^2) - 2\text{Log}(a - ix)}. \quad (\text{A2})$$

In the limit of a punctual source $a \rightarrow 0$, one gets $\Psi(x) = -i\sqrt{\text{Log}(1 - l^2/x^2)}$, where $x > 0$ is assumed for convenience. The concentration and velocity fields can be written explicitly by using the relation $\text{Log } z = \ln |z| + i \text{Arg } z$ for a complex number z .

The resulting steady state is illustrated in Fig. 6a. First, one can check that the flux of surfactant is constant from the source to the sink. Second, the concentration vanishes for $|x| > l$ whereas the velocity does not. This illustrates the non-local relation between concentration and velocity. Third, one can note the diverging slope of concentration and velocity profiles in the vicinity of sources and sinks. Finally, the concentration is clearly distinct from the linear profile expected with pure diffusion. The one-dimensional steady source with sinks is another situations where Marangoni spreading is not diffusive-like.

With evaporation. Evaporation acts as a distributed sink and presumably ensures the existence of a steady state. Even with the simplest case of a Cauchy source, the integration of Eq. (A1) leads to an equation on Ψ that is untractable. We can however look for an expansion of Ψ at small and large x . For small x , assuming $-i\Psi(x) = c_0 + c_1 ix + c_2 x^2$ with all coefficients real leads to an approximation that depends only on c_0 . One finds

$c_1 = 1/ac_0 - \alpha$ and $c_2 = (\alpha ac_0 + c_0^2 - 1)/(2a^2 c_0^3)$. The coefficient c_0 is solution of a transcendental equation that can only be solved numerically. In the vicinity of the source, the concentration profile is thus parabolic and the velocity profile is linear. For large x , assuming a power series $\Psi(x) = \sum_{n=1}^{\infty} c_n x^{-n}$ leads at lowest order to $\Psi(x) = 1/\alpha x - ia/\alpha x^2 + \dots$. Far from the source, the velocity and concentration fields decay as x^{-1} and x^{-2} respectively. Figure 6(b) shows a solution of Eq. (A1) obtained numerically, together with the approximations above. The latter are quite satisfactory, except for position around unity. Note finally that, consistent with the absence of steady solution when $\alpha = 0$, the limit of vanishing evaporation can not be taken.

Appendix B: Riesz transform of a radial function

Obtaining the Riesz transform is not straightforward, even with the assumption of radial symmetry. Accordingly, we give two expressions that we found useful in this purpose. From its definition in Fourier space of Eq. (42), the Riesz transform may be recast as

$$\check{f}(r) = -\partial_r \left[\mathcal{F}_{q \rightarrow r}^{-1} \left(\frac{1}{q} \mathcal{F}_{r \rightarrow q}(f(r)) \right) \right], \quad (\text{B1})$$

where \mathcal{F} indicates a Fourier transform for a purely radial two-dimensional function:

$$\mathcal{F}_{r \rightarrow q} f \equiv 2\pi \int_0^{\infty} f(r) J_0(qr) r dr, \quad (\text{B2a})$$

$$\mathcal{F}_{q \rightarrow r}^{-1} f \equiv \frac{1}{2\pi} \int_0^{\infty} f(q) J_0(qr) q dq, \quad (\text{B2b})$$

with J_m the Bessel function of the first kind of order m . An equivalent expression can be given in terms of Hankel transform [91]

$$\check{f}(r) = H_{1,q \rightarrow r}^{-1} [H_{0,r \rightarrow q} f(r)], \quad (\text{B3})$$

where H_ν is the Hankel transform of order ν :

$$H_{\nu,r \rightarrow q} f \equiv \int_0^{\infty} f(r) J_\nu(qr) r dr, \quad (\text{B4a})$$

$$H_{\nu,q \rightarrow r}^{-1} f \equiv \int_0^{\infty} f(q) J_\nu(qr) q dq. \quad (\text{B4b})$$

As a side remark, we note that the Riesz transform may be interpreted by analogy with electrostatic or gravitational field. If $f(r)$ is the radial density of charge on an infinitely thin disk, $\check{f}(r)$ is the radial component of the electric field in the plane of the disk. Let us then assume that identically charged particles are restricted to move in a plane and in a quiescent medium so that they have a fixed mobility, i.e. a linear relationship between their velocity and the force acting on them. Then, if non-electrostatic interaction can be neglected, the evolution of the charge density is governed by Eq. (44) and the process is analogous to Marangoni spreading.

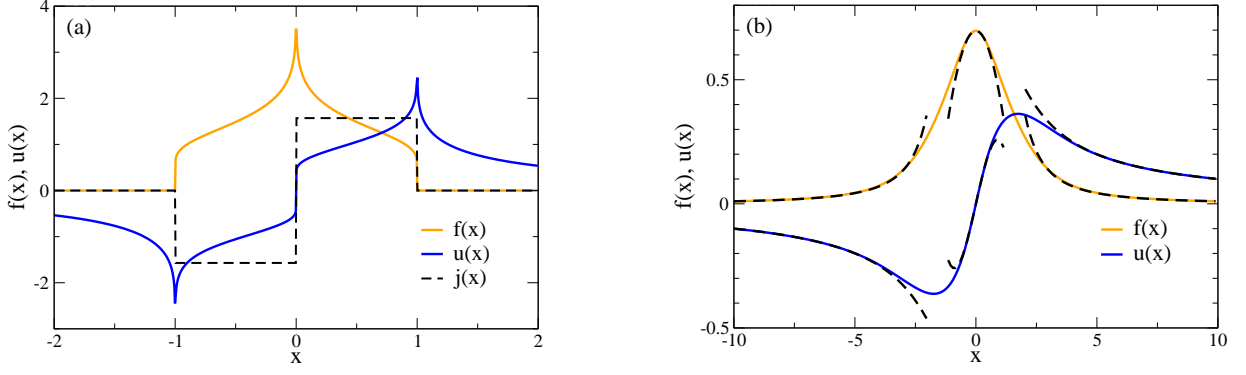


FIG. 6. Steady state around a source of surfactant. (a) Without evaporation. The punctual source at the origin is surrounded by two punctual sinks located at $x = l = \pm 1$. The dashed line is the local flux of surfactant $j(x) = u(x)f(x)$. (b) With evaporation. The source at the origin is of Cauchy type, with $a = 1$ and $\alpha = 1$. The dashed lines show the approximations at small and large x .

Appendix C: Long formulas

We give here some formulas that were too long to be included in the main body of the text in Sec. III B.

The Cauchy hole:

$$2t\Psi(x, t) = x + ia - i\bar{c}t - i\sqrt{a^2 - a(4\mathcal{A}t - 2\bar{c}t + 2ix) + (\bar{c}t - ix)^2}, \quad (\text{C1a})$$

$$f(x, t) = \frac{1}{2t}(\Upsilon^+ - a + \bar{c}t), \quad \Upsilon^\pm \equiv \sqrt{\sqrt{\xi^2 + (2(a + \bar{c}t)x)^2} \pm \xi/\sqrt{2}}, \quad (\text{C1b})$$

$$u(x, t) = \frac{1}{2t}(x - \Upsilon^-), \quad \xi \equiv a^2 + 2a(-2\mathcal{A} + \bar{c})t + \bar{c}^2t^2 - x^2. \quad (\text{C1c})$$

The circular hole:

$$\Psi(x, t) = \frac{\mathcal{A} \left(\sqrt{-a^2 + 2a\mathcal{A}t - (\bar{c}t - ix)^2} + i\bar{c}t - x \right) - ia\bar{c}}{a - 2\mathcal{A}t}, \quad (\text{C2a})$$

$$f(x, t) = \frac{\mathcal{A}}{2\mathcal{A}t - a}(\Upsilon^+ - a\bar{c}/\mathcal{A} + \bar{c}t), \quad \Upsilon^\pm \equiv \sqrt{\sqrt{\xi^2 + (2\bar{c}tx)^2} \pm \xi/\sqrt{2}}, \quad (\text{C2b})$$

$$u(x, t) = \frac{\mathcal{A}}{2\mathcal{A}t - a}(x - \Upsilon^-), \quad \xi \equiv a^2 - 2a\mathcal{A}t + \bar{c}^2t^2 - x^2. \quad (\text{C2c})$$

-
- [1] Matar, O. K., Craster, R. V., Dynamics of surfactant-assisted spreading. *Soft Matter* **5**, 3801 (2009).
 - [2] De Gennes, P., Brochard-Wyart, F., Quéré, D., *Capillarity and wetting phenomena: drops, bubbles, pearls, waves*, (Springer Verlag 2004).
 - [3] Scriven, L. E., Sterling, C. V., The Marangoni effects. *Nature* **187**, 186 (1960).
 - [4] Manikantan, H., Squires, T. M., Surfactant dynamics: Hidden variables controlling fluid flows. *J. Fluid Mech.* **892**, 1 (2020).
 - [5] Bel Fdhila, R. B., Duineveld, P. C., The effect of surfactant on the rise of a spherical bubble at high Reynolds and Peclet numbers. *Phys. Fluids* **8**, 310 (1996).
 - [6] Takagi, S., Matsumoto, Y., Surfactant effects on bubbly flows. *Annu. Rev. Fluid Mech.* **43**, 615 (2011).
 - [7] Palaparthi, R., Papageorgiou, D. T., Maldarelli, C., Theory and experiments on the stagnant cap regime in the motion of spherical surfactant-laden bubbles. *J. Fluid Mech.* **559**, 1 (2006).
 - [8] Crowdy, D. G., Exact solutions for the formation of stagnant caps of insoluble surfactant on a planar free surface. *J. Eng. Math.* **131** (2021).
 - [9] Peaudecerf, F. J., Landel, J. R., Goldstein, R. E., Luzzatto-Fegiz, P., Traces of surfactants can severely limit the drag reduction of superhydrophobic surfaces. *Proc. Natl. Acad. Sci. USA* **114**, 7254 (2017).
 - [10] Landel, J. R., Peaudecerf, F. J., Coletto, F. T., Gibou, F., Goldstein, R. E., Fegiz, P. L., A theory for the slip

- and drag of superhydrophobic surfaces with surfactant. *J. Fluid Mech.* **883**, A18 (2020).
- [11] Baier, T., Hardt, S., Influence of insoluble surfactants on shear flow over a surface in Cassie state at large Péclet numbers. *J. Fluid Mech.* **907**, A3 (2021).
- [12] Bickel, T., Effect of surface-active contaminants on radial thermocapillary flows. *Eur. Phys. J. E* **42**, 16 (2019).
- [13] Bickel, T., Loudet, J. C., Koleski, G., Pouligny, B., Hydrodynamic response of a surfactant-laden interface to a radial flow. *Phys. Rev. F* **4**, 124002 (2019).
- [14] Venerus, D. C., Nieto Simavilla, D., Tears of wine: New insights on an old phenomenon. *Sci. Rep.* **5**, 16162 (2015).
- [15] Trinschek, S., John, K., Thiele, U., Modelling of surfactant-driven front instabilities in spreading bacterial colonies. *Soft Matter* **14**, 4464 (2018).
- [16] Stetten, A. Z., Iasella, S. V., Corcoran, T. E., Garoff, S., Przybycienc, T. M., Tilton, R. D., Surfactant-induced Marangoni transport of lipids and therapeutics within the lung. *Curr. Opin. Colloid Interface Sci.* **36**, 58 (2018).
- [17] Botte, V., Mansutti, D., Numerical modelling of the Marangoni effects induced by plankton-generated surfactants. *J. Marine Syst.* **57**, 55 (2005).
- [18] Morciano, M., Fasano, M., Boriskina, S. V., Chiavazzo, E., Asinari, P., Solar passive distiller with high productivity and Marangoni effect-driven salt rejection. *Energy Environ. Sci.* **13**, 3646 (2020).
- [19] Quéré, D., Fluid coating on a fiber. *Annu. Rev. Fluid Mech.* **31**, 347 (1999).
- [20] Sauleda, M. L., Hsieh, T. L., Xu, W., Tilton, R. D., Garoff, S., Surfactant spreading on a deep subphase: Coupling of Marangoni flow and capillary waves. *J. Colloid Interface Sci.* **614**, 511 (2022).
- [21] Cantat, I., Cohen-Addad, S., Elias, F., Graner, F., Hohler, R., Pitois, O., Rouyer, F., Saint-James, A., *Foams - Structure and Dynamics*, (Oxford 2013).
- [22] Breward, C. J. W., Howell, P. D., The drainage of a foam lamella. *J. Fluid Mech.* **458**, 379 (2002).
- [23] Fei, W., Gu, Y., Bishop, K. J., Active colloidal particles at fluid-fluid interfaces. *Curr. Opin. Colloid Interface Sci.* **32**, 57 (2017).
- [24] Grosjean, G., Hubert, M., Collard, Y., Pillitteri, S., Vandewalle, N., Surface swimmers, harnessing the interface to self-propel. *Eur. Phys. J. E* **41**, 137 (2018).
- [25] Nakata, S., Pimienta, V., Lagzi, I., Kitahata, H., Suematsu, N. J., editors, *Self-organized motion: Physicochemical design based on nonlinear dynamics*, (RSC 2018).
- [26] Rednikov, A. Y., Ryazantsev, Y. S., Velarde, M. G., On the development of translational subcritical marangoni instability for a drop with uniform internal heat generation. *J. Colloid Interface Sci.* **164**, 168 (1994).
- [27] Boniface, D., Cottin-Bizonne, C., Kervil, R., Ybert, C., Detcherry, F., Self-propulsion of symmetric chemically active particles: Point-source model and experiments on camphor disks. *Phys. Rev. E* **99**, 062605 (2019).
- [28] Ender, H., Froin, A. K., Rehage, H., Kierfeld, J., Surfactant-loaded capsules as Marangoni microswimmers at the air-water interface: Symmetry breaking and spontaneous propulsion by surfactant diffusion and advection. *Eur. Phys. J. E* **44**, 21 (2021).
- [29] Suematsu, N. J., Nakata, S., Evolution of Self-Propelled Objects: From the Viewpoint of Nonlinear Science. *Chem. Eur. J.* **24**, 6308 (2018).
- [30] Nakata, S., Nagayama, M., Kitahata, H., Suematsu, N. J., Hasegawa, T., Physicochemical design and analysis of self-propelled objects that are characteristically sensitive to environments. *Phys. Chem. Chem. Phys.* **17**, 10326 (2015).
- [31] Dietrich, K., Jaensson, N., Buttinoni, I., Volpe, G., Isa, L., Microscale Marangoni surfers. *Phys. Rev. Lett.* **125**, 098001 (2020).
- [32] Boniface, D., Cottin-Bizonne, C., Detcherry, F., Ybert, C., Role of Marangoni forces in the velocity of symmetric interfacial swimmers. *Phys. Rev. F* **6**, 104006 (2021).
- [33] Suematsu, N. J., Sasaki, T., Nakata, S., Kitahata, H., Quantitative estimation of the parameters for self-motion driven by difference in surface tension. *Langmuir* **30**, 8101 (2014).
- [34] Kitahata, H., Yoshinaga, N., Effective diffusion coefficient including the Marangoni effect. *J. Chem. Phys.* **148**, 134906 (2018).
- [35] Bickel, T., Spreading dynamics of reactive surfactants driven by Marangoni convection. *Soft Matter* **15**, 3644 (2019).
- [36] Jensen, O. E., Grotberg, J. B., Insoluble surfactant spreading on a thin viscous film: Shock evolution and film rupture. *J. Fluid Mech.* **240**, 259 (1992).
- [37] Afsar-Siddiqui, A. B., Luckham, P. F., Matar, O. K., The spreading of surfactant solutions on thin liquid films. *Adv. Colloid Interface Sci.* **106**, 183 (2003).
- [38] Dussaud, A. D., Matar, O. K., Troian, S. M., Spreading characteristics of an insoluble surfactant film on a thin liquid layer: Comparison between theory and experiment. *J. Fluid Mech.* **544**, 23 (2005).
- [39] Craster, R. V., Matar, O. K., Dynamics and stability of thin liquid films. *Rev. Mod. Phys.* **81**, 1131 (2009).
- [40] Swanson, E. R., Strickland, S. L., Shearer, M., Daniels, K. E., Surfactant spreading on a thin liquid film: reconciling models and experiments. *J. Eng. Math.* **94**, 63 (2015).
- [41] Jensen, O. E., The spreading of insoluble surfactant at the free surface of a deep fluid layer. *J. Fluid Mech.* **293**, 349 (1995).
- [42] Roché, M., Li, Z., Griffiths, I. M., Le Roux, S., Cantat, I., Saint-Jalmes, A., Stone, H. A., Marangoni flow of soluble amphiphiles. *Phys. Rev. Lett.* **112**, 208302 (2014).
- [43] Le Roux, S., Roché, M., Cantat, I., Saint-Jalmes, A., Soluble surfactant spreading: How the amphiphilicity sets the Marangoni hydrodynamics. *Phys. Rev. E* **93**, 013107 (2016).
- [44] Bandi, M., Akella, V., Singh, D., Singh, R., Mandre, S., Hydrodynamic signatures of stationary Marangoni-driven surfactant transport. *Phys. Rev. Lett.* **119**, 264501 (2017).
- [45] Mandre, S., Axisymmetric spreading of a surfactant driven by self-imposed Marangoni stress under simplified transport. *J. Fluid Mech.* **832**, 777 (2017).
- [46] Thess, A., Spirn, D., Jüttner, B., Viscous flow at infinite Marangoni number. *Phys. Rev. Lett.* **75**, 4614 (1995).
- [47] Crowdy, D. G., Viscous Marangoni flow driven by insoluble surfactant and the complex Burgers equation. *SIAM J. Appl. Math.* **81**, 2526 (2021).
- [48] Shmyrov, A., Mizev, A., Surface diffusion in gaseous monolayers of an insoluble surfactant. *Langmuir* **35**, 14180 (2019).
- [49] Thess, A., Spirn, D., Jüttner, B., A two-dimensional model for slow convection at infinite Marangoni number. *J. Fluid Mech.* **331**, 283 (1997).

- [50] Kralchevsky, P. A., Danov, K. D., Chemical physics of colloid systems and interfaces, in Birdi, K. S., editor, *Handbook of surface and colloid chemistry*, (CRC Press 2016).
- [51] Pawar, Y., Stebe, K. J., Droplet deformation in an extensional flow: the role of surfactant physical chemistry. *Phys. Fluids* **8**, 1738 (1996).
- [52] Thess, A., Stokes flow at infinite Marangoni number: exact solutions for the spreading and collapse of a surfactant. *Phys. Scr.* **T67**, 96 (1996).
- [53] Pismen, L. M., Interaction of reaction-diffusion fronts and Marangoni flow on the interface of a deep fluid. *Phys. Rev. Lett.* **78**, 382 (1997).
- [54] Constantin, P., Lax, P. D., Majda, A., A simple one-dimensional model for the three-dimensional vorticity equation. *Commun. Pure Appl. Math.* **38**, 715 (1985).
- [55] King, F. W., *Hilbert transforms*, (Cambridge 2009).
- [56] Burgers, J. M., *The nonlinear diffusion equation*, (Springer, Dordrecht 1974).
- [57] Bonkile, M. P., Awasthi, A., Lakshmi, C., Mukundan, V., Aswin, V. S., A systematic literature review of Burgers' equation with recent advances. *Pramana - J. Phys.* **90**, 69 (2018).
- [58] Hopf, E., The partial differential equation $u_t + uu_x = \mu u_{xx}$. *Commun. Pure Appl. Math.* **3**, 201 (1950).
- [59] Whitham, G. B., *Linear and Nonlinear Waves*, (Wiley, New York 1974).
- [60] Arfken, G., Weber, H., *Mathematical methods for physicists*, volume 3, (Academic press New York 2005).
- [61] To separate the real and imaginary part, one can use the relation $\sqrt{2}\sqrt{x+iy} = \sqrt{\rho+x} + i \operatorname{sign}(y)\sqrt{\rho-x}$, where x and y are reals and $\rho = \sqrt{x^2+y^2}$.
- [62] Biler, P., Imbert, C., Karch, G., Barenblatt profiles for a nonlocal porous medium equation. *C. R. Acad. Sci. Paris, Ser. I* **349**, 641 (2011).
- [63] Barenblatt, G., *Scaling, self-similarity and intermediate asymptotics*, (Cambridge Univ Press 1997).
- [64] Pattle, R. E., Diffusion from an instantaneous point source with a concentration-dependent coefficient. *Quarterly J. Mech. Appl. Math.* **12**, 407 (1959).
- [65] The derivative of a Cauchy pulse leads to a third-order equation that is also solvable.
- [66] In the sense that the norm of the difference between the solution and the circular solution tends toward zero at large time, that is $\|f(x,t) - f_c(x,t)\|_p \rightarrow 0$ for $t \rightarrow \infty$, with $\|\cdot\|_p$ a p -norm.
- [67] Xu, Y., Takayama, N., Komatsu, Y., Takahara, N., Kitahata, H., Iima, M., Nakata, S., Self-propelled camphor disk dependent on the depth of the sodium dodecyl sulfate aqueous phase. *Colloids Surf. A* **635**, 128087 (2022).
- [68] For the concentration to remain positive, one should have $0 \leq \mathcal{A} \leq \bar{c}$.
- [69] Corless, R. M., Gonnet, G. H., Hare, D. E., Jeffrey, D. J., Knuth, D. E., On the Lambert W function. *Adv. Comput. Math.* **5**, 329 (1996).
- [70] A Hubbard-Stratonovitch transform is first introduced for the exponential term. After switching the integration order, the double integral can also be obtained.
- [71] Gradshteyn, I., Ryzhik, I., *Table of integrals, series, and products*, (Academic Press, London 2007).
- [72] $C_1 = -(\gamma_E + \psi^{(0)}(1/2))/2\pi$, with γ_E Euler's constant and ψ a polygamma function.
- [73] Remember that we set $a\mathcal{A} = 1/\pi$ and take the limit $a \rightarrow 0$.
- [74] Arangalage, M., Li, X., Lequeux, F., Talini, L., Dual Marangoni effects and detection of traces of surfactants. *Soft Matter* **14**, 3378 (2018).
- [75] Benouaguef, I., Musunuri, N., Amah, E. C., Blackmore, D., Fischer, I. S., Singh, P., Solutocapillary Marangoni flow induced in a waterbody by a solute source. *J. Fluid Mech.* **922**, A23 (2021).
- [76] Equation (42) depends on the convention chosen for the definition of Fourier transform.
- [77] Bratukhin, Y. K., Maurin, L. M., Thermocapillary convection in a fluid filling a half-space. *J. Appl. Math. Mech.* **31**, 605 (1967).
- [78] Shtern, V. N., Hussain, F., Azimuthal instability of divergent flows. *J. Fluid Mech.* **256**, 535 (1993).
- [79] Whether in a specific experiment the surfactant may actually be considered as insoluble depends on a number of factors, including the characteristic time for desorption from the interface, the time over which spreading is observed and the initial concentration of surfactant [44].
- [80] $\chi = 1$ and 2 for Cauchy and circular cases respectively.
- [81] Grotberg, J. B., Halpern, D., Jensen, O. E., Interaction of exogenous and endogenous surfactant: Spreading-rate effects. *J. Appl. Physiol.* **78**, 750 (1995).
- [82] Sauleda, M. L., Chu, H. C., Tilton, R. D., Garoff, S., Surfactant-driven Marangoni spreading in the presence of predeposited insoluble surfactant monolayers. *Langmuir* **37**, 3309 (2021).
- [83] Mcnair, R., Jensen, O. E., Landel, J. R., Surfactant spreading in a two-dimensional cavity and emergent contact-line singularities. *J. Fluid Mech.* **930**, A15 (2022).
- [84] Shardt, O., Masoud, H., Stone, H. A., Oscillatory Marangoni flows with inertia. *J. Fluid Mech.* **803**, 94 (2016).
- [85] Fallest, D. W., Lichtenberger, A. M., Fox, C. J., Daniels, K. E., Fluorescent visualization of a spreading surfactant. *New J. Phys.* **12**, 073029 (2010).
- [86] Usma, C. L., Mariot, S., Goldmann, C., Roch, M., Salonen, A., Tresset, G., Fluorescent Marangoni flows under quasi-steady conditions. *Langmuir* **38**, 9129 (2022).
- [87] Eastoe, J., Vesperinas, A., Self-assembly of light-sensitive surfactants. *Soft Matter* **1**, 338 (2005).
- [88] Liu, X., Abbott, N. L., Spatial and temporal control of surfactant systems. *J. Colloid Interface Sci.* **339**, 1 (2009).
- [89] Chevallier, E., Saint-Jalmes, A., Cantat, I., Lequeux, F., Monteux, C., Light induced flows opposing drainage in foams and thin-films using photosurfactants. *Soft Matter* **9**, 7054 (2013).
- [90] Kavokine, N., Anyfantakis, M., Morel, M., Rudiuk, S., Bickel, T., Baigl, D., Light-driven transport of a liquid marble with and against surface flows. *Angew. Chem., Int. Ed.* **55**, 11183 (2016).
- [91] The expression holds provided all involved integrals are convergent.